

## MAS-NMR Studies of Carbonate Retention in a Very Wide Range of Na<sub>2</sub>O-SiO<sub>2</sub> Glasses

BARROW, Nathan, PACKARD, Michael, VAISHNAV, Shuchi, WILDING, Martin, BINGHAM, Paul <<http://orcid.org/0000-0001-6017-0798>>, HANNON, Alex, APPLER, Matthew and FELLER, Steve

Available from Sheffield Hallam University Research Archive (SHURA) at:

<http://shura.shu.ac.uk/25762/>

---

This document is the author deposited version. You are advised to consult the publisher's version if you wish to cite from it.

### Published version

BARROW, Nathan, PACKARD, Michael, VAISHNAV, Shuchi, WILDING, Martin, BINGHAM, Paul, HANNON, Alex, APPLER, Matthew and FELLER, Steve (2020). MAS-NMR Studies of Carbonate Retention in a Very Wide Range of Na<sub>2</sub>O-SiO<sub>2</sub> Glasses. *Journal of Non-Crystalline Solids*, 534, p. 119958.

---

### Copyright and re-use policy

See <http://shura.shu.ac.uk/information.html>

# MAS-NMR Studies of Carbonate Retention in a Very Wide Range of Na<sub>2</sub>O-SiO<sub>2</sub> Glasses

Nathan Barrow<sup>a</sup>, Michael Packard<sup>b</sup>, Shuchi Vaishnav<sup>c</sup>, Martin C. Wilding<sup>c</sup>, Paul A. Bingham<sup>c</sup>, Alex C. Hannon<sup>d</sup>, Matthew Appler<sup>b</sup> and Steve Feller<sup>b</sup>

<sup>a</sup> *Johnson Matthey Technology Centre, Blount's Court, Sonning Common, Reading, RG4 9NH, UK*

<sup>b</sup> *Physics Department, Coe College, Cedar Rapids, IA 52402, USA*

<sup>c</sup> *Materials and Engineering Research Institute, Faculty of Science, Technology and Arts, Sheffield Hallam University, Sheffield, S1 1WB, UK*

<sup>d</sup> *ISIS Facility, Rutherford Appleton Laboratory, Chilton, Didcot, Oxon, OX11 0QX, UK*

## Abstract

Glasses that contain carbon are of geological interest, and the form of that carbon can be probed by Magic-Angle Spinning Nuclear Magnetic Resonance (MAS-NMR) spectroscopy. Previous studies of the Na<sub>2</sub>O-SiO<sub>2</sub> glass system could only reach 56 mol% Na<sub>2</sub>O. Here we reproduce and extend those studies to cover a very wide compositional range, from 20 to 70 mol% Na<sub>2</sub>O, by using a combination of conventional melt-quench and twin roller quenching technologies on natural and 99% <sup>13</sup>C-enriched sodium silicate glasses. <sup>13</sup>C MAS-NMR reveals that measurable levels of carbon retention occur above at least 40 mol% Na<sub>2</sub>O, and takes the form of CO<sub>3</sub><sup>2-</sup> ions incorporated in the glass structure. These CO<sub>3</sub><sup>2-</sup> anions are surrounded by Na<sup>+</sup> cations, forming nanoscale domains in a sodium silicate glass network. <sup>23</sup>Na MAS-NMR showed a linear decrease in mean Na—O bond length with increasing Na<sub>2</sub>O content, up to 60 mol% Na<sub>2</sub>O, above which the mean Na—O bond length increased. Elemental analysis detected significant (>5%) carbonate by mass in the 65 and 70 mol% Na<sub>2</sub>O glasses. For the 70 mol% Na<sub>2</sub>O glass, <sup>13</sup>C and <sup>23</sup>Na MAS-NMR detected ordered nanoscale domains composed of only Na<sub>2</sub>O and CO<sub>2</sub>. These results have shown the quantity and nature of carbon retention in the archetypal sodium silicate glass system, which will better inform structural models and carbonate solubility limits.

## I. Introduction

Sodium silicate glass is the archetypical simple glass-forming system and is pivotal to our fundamental understanding of glass science. Sodium silicate forms the basis of many important glass applications such as flat glass, automobile glass, window glass, Pyrex and other borosilicates, bioglass, ion-strengthened glasses, and numerous industrial glasses<sup>1-3</sup>. Yet for all its practical import the studied regime for these glasses is typically between 20 mol% and 50 mol% Na<sub>2</sub>O. This is so because of phase separation and high liquidus temperatures and viscosities below 20 mol% Na<sub>2</sub>O, and crystallization above 50 mol% Na<sub>2</sub>O when the melt is cooled relatively slowly.

The conventional structural short-range model for the silicate network in the sodium silicate glass system is the *Lever-rule Model*<sup>4</sup>. The short-range structure is described by Q<sub>n</sub> units where Q is a silicate tetrahedron and n is the number of bridging oxygens. The glasses proceed from Q<sub>4</sub> to Q<sub>0</sub> with a simplified binary model of Q<sub>n</sub> transforming to Q<sub>n-1</sub> as Na<sub>2</sub>O content increases. Each Q unit has 4-n nearby sodium ions for charge balance. Thus, the charge of the Q<sub>n</sub> tetrahedron is  $-(4-n) = n-4$ .

Previous studies have considered glasses containing up to 56 mol% Na<sub>2</sub>O<sup>4</sup>. Through our access to twin-roller rapid quenching, for the first time we have been able to form and characterize Na<sub>2</sub>O-SiO<sub>2</sub> glasses to 70 mol% Na<sub>2</sub>O. We have performed the most comprehensive study of the structure and property of these glasses across the widest compositional range to date, namely 20 mol% to 70 mol% Na<sub>2</sub>O by batch. These results are being reported in a series of linked papers, of which this is the first, covering a wide range of complementary techniques including neutron and X-ray diffraction, Raman and infrared spectroscopies, density, molar volume, atomic packing and thermal analysis, carbon elemental assay, and <sup>13</sup>C, <sup>23</sup>Na and <sup>29</sup>Si MAS-NMR.

Here we focus on carbonate retention and structural aspects using a combination of carbon elemental assay and <sup>13</sup>C / <sup>23</sup>Na high-field magic angle spinning nuclear magnetic resonance (MAS-NMR) studies. The <sup>29</sup>Si MAS-NMR results will be reported in a later paper and have been used to confirm and extend to new compositions beyond what has been reported for the structural evolution of the Q<sub>n</sub> species. The diffraction data and the vibrational spectroscopy that will be presented in the linked papers will give supporting evidence for the Lever-rule model as well as the effects of carbonate retention on the structure. The various measures derived from density will be used to show how physical property data are influenced by short-range structure.

Substantial carbonate retention occurs in all alkali-containing oxide glass systems above a certain threshold alkali concentration<sup>5,6,7</sup>. For example, for lithium borosilicate glass, RLi<sub>2</sub>O.B<sub>2</sub>O<sub>3</sub>.KSiO<sub>2</sub>, experiment and a model show that carbonate retention begins<sup>5</sup> near an R value of 3 + 2K. For the sodium borate case the retention begins near<sup>6</sup> R = 2 in RNa<sub>2</sub>O.B<sub>2</sub>O<sub>3</sub> and this causes glass formation to be enhanced above the orthoborate composition. The structural role of the carbonate has been unknown to date and is a thrust of the present paper.

## II. Experimental Procedures

### a. Sample preparation.

This investigation covers two sets of samples, one made with natural abundance  $\text{Na}_2\text{CO}_3$  and one with 99%  $^{13}\text{C}$  enriched  $\text{Na}_2\text{CO}_3$ . The  $^{13}\text{C}$ -enriched samples were also doped with a 0.1 wt% iron oxide ( $\text{Fe}_2\text{O}_3$ ) to decrease the NMR relaxation time without affecting the peak widths or shifts<sup>8</sup>. Both sets of samples were synthesised under comparable conditions, and the melting process was identical for the corresponding samples from each set. Amorphous samples of nominal  $x\text{Na}_2\text{O}\cdot(1-x)\text{SiO}_2$  compositions of  $x = 0.20, 0.25, 0.30, 0.35, 0.40$  and  $0.45$  were produced by conventional melt quenching at Sheffield Hallam University, UK. The  $x = 0.50$  glass crystallised upon cooling. A second attempt using splat quenching resulted in a partially amorphous sample. Glassy samples of composition  $x = 0.45, 0.50, 0.55, 0.60, 0.65,$  and  $0.70$  were made at Coe College, USA, using either plate quenching or a twin roller quencher, inside a dry nitrogen glove box. All of these samples had natural abundance carbon from sodium carbonate. Samples with  $^{13}\text{C}$  enrichment were made at Coe College and had compositions of  $x = 0.20, 0.25, 0.30, 0.35, 0.40, 0.45, 0.50, 0.55, 0.60, 0.65,$  and  $0.70$ .

The starting materials at both Coe College and Sheffield Hallam University were  $\text{Na}_2\text{CO}_3$  (natural abundance carbon) and  $\text{SiO}_2$  of reagent grade (>99.9%) or higher purity. 99% purity  $^{13}\text{C}$ -enriched  $\text{Na}_2\text{CO}_3$  was obtained from Cambridge Isotopes (Cambridge, Massachusetts, USA). Sodium carbonate was employed to provide a source of carbonate to be retained in the glasses. All reagents were well mixed and fused in platinum crucibles at temperatures ranging from 1140 °C to 1550 °C, with the higher temperatures necessary to melt the lower-sodium content glasses.

At Sheffield Hallam University batch compositions were prepared for 125g of glass using a calibrated balance with precision of  $\pm 0.001$  g, mixed thoroughly, and melted in a Pt-ZGS (ZrO<sub>2</sub> Grain Stabilized) crucible loosely covered with a Pt-ZGS lid to reduce  $\text{Na}_2\text{O}$  volatilization losses and contamination. The melts were attained within a temperature range of 1300-1470 °C (depending upon liquidus temperature and viscosity, as determined from appropriate phase diagrams and glass data), with a dwell time of 3 hours per melt, then poured onto a clean steel plate and allowed to cool gradually to room temperature. The glasses were not annealed. The cooled glasses were then immediately transferred into a vacuum desiccator to avoid hydration, in consideration of their limited chemical durability, particularly at lower  $\text{SiO}_2$  contents. See Table 1 for additional details.

Samples made at Coe College were heated twice in pure platinum crucibles, and before the second heating a weight loss measurement was performed to check for carbonate retention. As above, the melt temperature range was 1140-1550 °C (depending upon liquidus temperature and viscosity as determined from appropriate phase diagrams and glass data), with a total heating time of approximately 25 minutes. Weight losses at high  $\text{Na}_2\text{O}$  contents that are below the predicted values, indicative of carbonate retention, were observed. Since clear, colorless, and bubble free samples were obtained in all cases, these melting times were found to be adequate.

Table 1 summarizes the preparation of the samples.

a. Natural C samples

Sample Source	$x\text{Na}_2\text{O}$ Composition (Mol. Fraction)	Heating Temperature ( $^{\circ}\text{C}$ )	Glass Weight (g)	Time (min)
Sheffield-Hallam	0.20	1470	125	180
Sheffield-Hallam	0.25	1430	125	180
Sheffield-Hallam	0.30	1380	125	180
Sheffield-Hallam	0.35	1350	125	180
Sheffield-Hallam	0.40	1330	125	180
Sheffield-Hallam	0.45	1300	125	180
Sheffield-Hallam	0.50	1260	125	180
Coe College	0.45	1200	6	25
Coe College	0.50	1200	6	25
Coe College	0.55	1200	6	25
Coe College	0.60	1200	6	25
Coe College	0.65	1140	6	25
Coe College	0.70	1140	6	25

b.  $^{13}\text{C}$  enriched samples

Sample Source	$x\text{Na}_2\text{O}$ Composition (Mol. Fraction)	$\text{Fe}_2\text{O}_3$ content (g)	Heating Temperature ( $^{\circ}\text{C}$ )	Glass Weight (g)	Time (min)
Coe College	0.20	0.006	1550	6	25
Coe College	0.25	0.006	1450	6	25
Coe College	0.30	0.007	1450	6	25
Coe College	0.35	0.006	1350	6	25
Coe College	0.40	0.006	1350	6	25
Coe College	0.45	0.006	1200	6	25
Coe College	0.50	0.006	1200	6	25
Coe College	0.55	0.006	1200	6	25
Coe College	0.60	0.006	1200	6	25
Coe College	0.65	0.006	1140	6	25
Coe College	0.70	0.006	1140	6	25

Table 1. Formation details for the sodium silicate glasses

b. Carbon elemental assay

Carbon elemental assay was employed using a LECO CS844ES combustion furnace to measure the carbon content in the samples. The bulk glasses were crushed and milled at 700 rpm for a minute to produce glass powders. The powders were combusted in a high frequency induction furnace in the presence of pure  $\text{O}_2$  gas until complete combustion was achieved. The analyses were carried out by an ISO 17025 (UKAS) accredited testing facility and the instrument was calibrated using appropriate Certified Reference Materials (CRMs). The range of calibrations covered all of the samples analyzed here, and additionally other CRMs were run as samples to confirm the calibration. These acted as independent validation of the calibration. Measurement uncertainties are provided as a percentage of the amount of carbon present in the sample, as

follows (% C in sample / % uncertainty of measured value): 3/2, 1/5, 0.2/5, <0.10/10, <0.005/20. The detection limit for these analyses was < 10 ppm (< 0.001%).

c.  $^{13}\text{C}$  and  $^{23}\text{Na}$  MAS-NMR experimental details

Solid-state MAS-NMR spectra were acquired at a static magnetic field strength of 14.1 T ( $\nu_0(^1\text{H}) = 600$  MHz) on a Bruker Avance Neo console using TopSpin 4.0 software. A wide bore Bruker 4 mm MAS probe was used. For  $^{13}\text{C}$ , the probe was tuned to 150.95 MHz and referenced to alanine  $\text{CH}_3$  at 20.5 ppm. For  $^{23}\text{Na}$ , the probe was tuned to 158.77 MHz and referenced to NaCl at 7.28 ppm. The glass pieces were ground by hand and packed into zirconia MAS rotors with Kel-F caps, in a dry nitrogen glovebox. Before and after weight measurements provided the sample mass for intensity normalization. Sodium carbonate was measured as received. The rotors were spun at 10 kHz for  $^{13}\text{C}$  and 14 kHz for  $^{23}\text{Na}$ , using room-temperature purified compressed air. Nutation tip angle was  $90^\circ$  for  $^{13}\text{C}$ , and  $45^\circ$  for  $^{23}\text{Na}$ . Relaxation times, unless otherwise stated, were 1000 s for  $^{13}\text{C}$  and 0.01 s for  $^{23}\text{Na}$ . To check for non-homogeneous distribution of  $\text{Fe}_2\text{O}_3$  in the glass, saturation recovery experiments were performed. For the amorphous phase, there was no  $^{23}\text{Na}$  line shape change between 0.01 s, 0.25 s and 10 s relaxation times. The locally ordered carbonate peaks continued to grow relative to the amorphous phase peak. Similarly, for the  $^{13}\text{C}$  MAS-NMR, the more ordered carbonate had a much longer relaxation time than the amorphous phase. There was no indication of differential relaxation occurring in the  $^{23}\text{Na}$  and  $^{13}\text{C}$  spectra, which would manifest as a multi-exponential relaxation rate. For  $^{13}\text{C}$ , between 4 and 32 scans were acquired using a one pulse acquisition program. For  $^{23}\text{Na}$ , 8192 scans were acquired using a Hahn echo pulse sequence.  $^{29}\text{Si}$  MAS-NMR details will be provided in a future paper in this series.

### III. Results

a. Carbon elemental assay

Carbon retention in this glass system was quantified by LECO combustion furnace elemental analysis. At nominal compositions  $x = 0.20, 0.25, 0.30,$  and  $0.35$   $\text{Na}_2\text{O}$  there was no more than 0.0001 weight fraction carbon detection. There was greater carbon retention with composition, and at the highest three compositions by  $\text{Na}_2\text{O}$  content, significant amounts of carbon were detected. At  $x = 0.60$   $\text{Na}_2\text{O}$  by batch the carbon detection was 0.0027 weight fraction, at  $x = 0.65$   $\text{Na}_2\text{O}$  the carbon detection was 0.0147 weight fraction, and at  $x = 0.70$   $\text{Na}_2\text{O}$  the carbon detection was 0.0305 weight fraction. To obtain the amount of carbon dioxide in the glasses we took the carbon assay results and converted to carbon dioxide concentration by

$$\begin{aligned} \text{Weight fraction CO}_2 &= w_{\text{C}}M_{\text{CO}_2}/M_{\text{C}} \\ &= 3.664w_{\text{C}} \end{aligned} \quad (1)$$

where  $w_{\text{C}}$  is the detected weight fraction of carbon, and  $M_{\text{CO}_2}$  and  $M_{\text{C}}$  are the masses of  $\text{CO}_2$  and C respectively. The weight fraction of  $\text{CO}_2$  is plotted as a function of  $x$  in Figure 1. The onset of significant amounts of carbon dioxide retention is at approximately  $x = 0.60$   $\text{Na}_2\text{O}$ . It is noted that the samples containing 45 and 50 molar percent sodium oxide yielded closely similar

carbonate retention for samples prepared at Coe and Sheffield Hallam, consistent with the view that both sample preparation methods used in this paper yielded closely similar levels of carbonate retention in the final glasses, and consequently that CO<sub>2</sub> evolution during melting did not significantly differ between the two preparation approaches used.

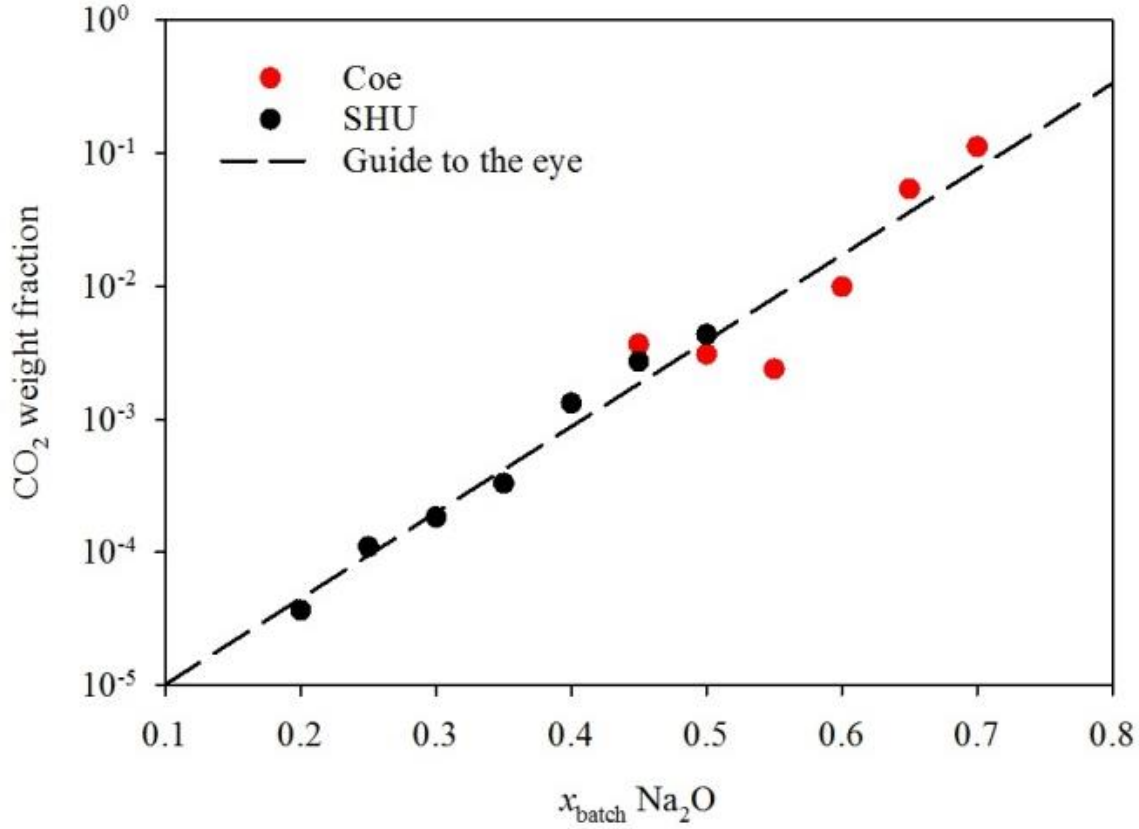


Figure 1. Weight fraction of CO<sub>2</sub> as a function of  $x$  on a semi-log plot. The dashed line is a guide to the eye.

Now that we have shown carbon is retained, we can correct the batch soda concentration to account for this retention. For this, we use the molar ratio  $J$  as a compositional parameter, where:

$$J = \frac{\text{Na}_2\text{O molar percent}}{\text{SiO}_2 \text{ molar percent}} \quad (2)$$

For a binary glass of composition  $x\text{Na}_2\text{O} \cdot (1-x)\text{SiO}_2$ , the molar ratio is:

$$J = \frac{x}{1-x} \quad (3)$$

The molar ratio,  $J_C$ , corrected for carbon retention (weight fraction  $w_C$ ) was determined as follows: Consider a batch prepared with composition  $J_{\text{batch}}(\text{Na}_2\text{CO}_3) \cdot \text{SiO}_2$ . Upon heating carbon dioxide is released, and if there is no carbon retention then a glass of composition  $J_{\text{batch}}\text{Na}_2\text{O} \cdot \text{SiO}_2$  is formed. However, a fraction  $f_C$  of the carbon atoms is retained (and two oxygen atoms are also retained for each carbon atom), with the result that the cooled glass actually has the following composition



This formula can be re-written as follows

$$J_C(\text{Na}_2\text{O}) \cdot f_C J_{\text{batch}}(\text{Na}_2\text{CO}_3) \cdot \text{SiO}_2, \text{ where } J_C = J_{\text{batch}}(1 - f_C). \quad (5)$$

The LECO measurement provides the weight fraction of carbon in the glass,  $w_C$ , given by

$$w_C = \frac{f_C J_{\text{batch}} M_C}{J_{\text{batch}} M_{\text{Na}_2\text{O}} + f_C J_{\text{batch}} M_{\text{CO}_2} + M_{\text{SiO}_2}} \quad (6)$$

where  $M_C$ ,  $M_{\text{SiO}_2}$ ,  $M_{\text{Na}_2\text{O}}$ , and  $M_{\text{CO}_2}$  are the respective molecular masses. Re-arranging equation (6) gives

$$f_C = \frac{w_C (J_{\text{batch}} M_{\text{Na}_2\text{O}} + M_{\text{SiO}_2})}{J_{\text{batch}} (M_C - w_C M_{\text{CO}_2})} \quad (7)$$

Equation (7) allows us to use the LECO measurement of  $w_C$  to calculate the fraction of carbon that is retained. The resulting net modifications are shown in Table 2, as both corrected molar fractions of  $\text{Na}_2\text{O}$  and corrected  $J_C$  values. Figure 2 displays  $J_C$  vs  $J_{\text{Batch}}$ .

<b>Batch <math>x\text{Na}_2\text{O}</math> Content (Molar Fraction)</b>	<b><math>J_{\text{Batch}}</math></b>	<b>Weight Fraction Carbon <math>w_C</math> from LECO Analysis</b>	<b>Weight Fraction Carbon Dioxide from LECO Analysis</b>	<b><math>J_C</math></b>	<b>Corrected Molar Fraction (<math>x</math>) of <math>\text{Na}_2\text{O}</math> from LECO Analysis</b>
0.70	2.333	0.0305	0.112	1.748	0.636
0.65	1.857	0.0147	0.054	1.631	0.620
0.60	1.500	0.0027	0.010	1.465	0.594
0.55	1.222	0.00065	0.002	1.215	0.549
0.50 (made at Coe)	1.000	0.00084	0.003	0.991	0.498
0.50 (made at SHU)	1.000	0.00118	0.004	0.988	0.497
0.45 (made at Coe)	0.818	0.00100	0.004	0.809	0.447
0.45 (made at SHU)	0.818	0.00074	0.003	0.811	0.448
0.40	0.667	0.00036	0.001	0.664	0.399
0.35	0.538	0.00009	0.000	0.538	0.350
0.30	0.429	0.00005	0.000	0.428	0.300
0.25	0.333	0.00003	0.000	0.331	0.250



0.20	0.250	0.00001	0.000	0.250	0.200
------	-------	---------	-------	-------	-------

Table 2: Effects of carbonate retention on compositions of sodium silicate glasses

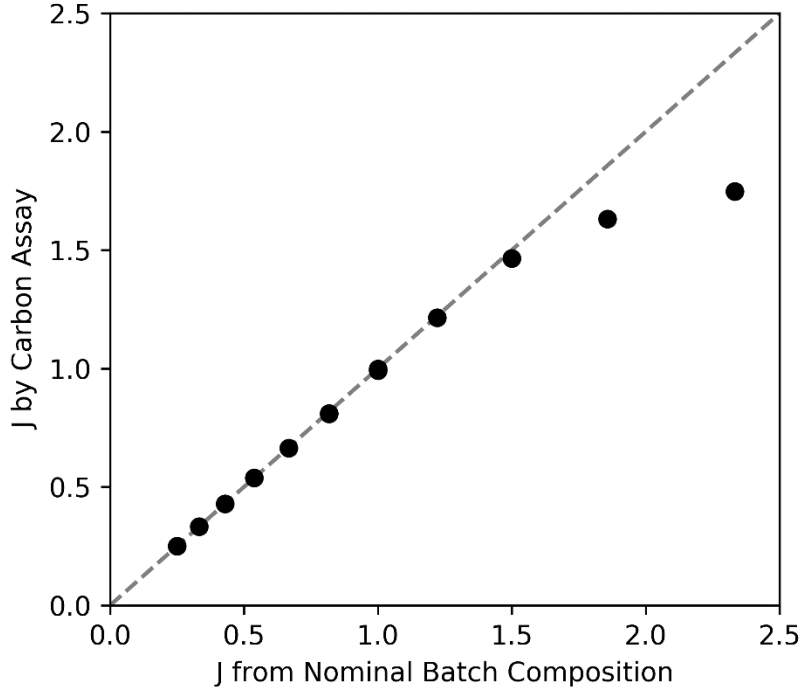


Figure 2:  $J_C$ ,  $J$  corrected for carbon retention, as a function of  $J_{\text{batch}}$ .

The deviation between  $J_C$  and  $J_{\text{batch}}$  near  $J = 1.5$  (60 mol%  $\text{Na}_2\text{O}$ ) in Figure 2 is due to carbonate retention. To shed light on the nature of the retained carbon, we applied  $^{13}\text{C}$  MAS-NMR.

#### b. Carbon and Sodium MAS-NMR

$^{13}\text{C}$  MAS-NMR spectra from  $^{13}\text{C}$  enriched samples are given in Figure 3 and clearly show the presence of carbon retention, in agreement with the elemental analysis results. From the chemical shift, we see that the carbon is present in the glasses in the form of  $\text{CO}_3^{2-}$ , rather than as dissolved  $\text{CO}_2$  (or  $\text{CO}_2$  gas trapped in bubbles).<sup>9</sup> No carbon-silicon species were detected either, which would typically be expected to appear at approximately 20 ppm chemical shift<sup>10</sup>. In general, these NMR results show that more carbonate was retained for greater soda contents, consistent with the results of carbon elemental assay. Notably,  $^{13}\text{C}$  MAS NMR was able to clearly detect the presence of carbonate even as low as  $x = 0.40$ . Up to 65 mol%  $\text{Na}_2\text{O}$ , the carbonate was all present in a locally disordered form as indicated by the presence of a broad (2 ppm FWHM) peak centered around 171.6 ppm.

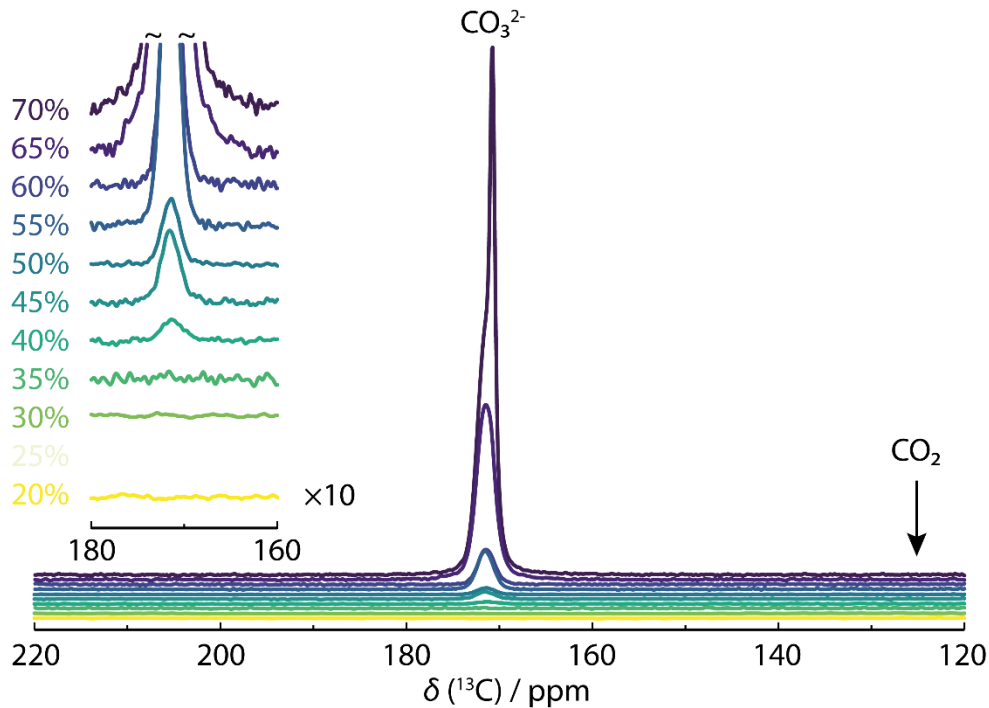


Figure 3. Normalized  $^{13}\text{C}$  MAS-NMR spectra of  $\text{Na}_2\text{O-SiO}_2$  glasses prepared using 99%  $^{13}\text{C}$ -enriched  $\text{Na}_2\text{CO}_3$ . Percentages indicate nominal glass composition in mol%  $\text{Na}_2\text{O}$ . Data for the 25 mol%  $\text{Na}_2\text{O}$  sample was not acquired for time efficiency as no signal was obtained for the 30 mol%  $\text{Na}_2\text{O}$  sample. The labels  $\text{CO}_3^{2-}$  and  $\text{CO}_2$  represent locations for the chemical shift of those respective species.

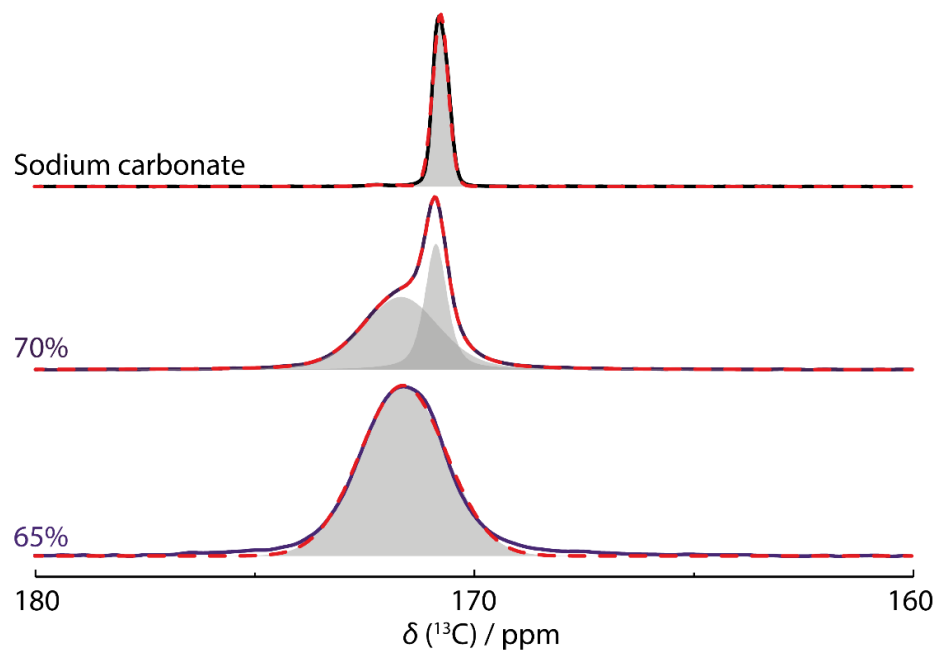


Figure 4.  $^{13}\text{C}$  MAS NMR spectra of high soda  $\text{Na}_2\text{O-SiO}_2$  glasses prepared using 99%  $^{13}\text{C}$ -enriched  $\text{Na}_2\text{CO}_3$ , along with a spectrum for pure crystalline  $\text{Na}_2\text{CO}_3$ . Grey shapes are peak fits,

red dashed lines represent the sum of the fits. Spectra are not normalized, but scaled to the same height.

By analyzing the  $^{13}\text{C}$  MAS-NMR spectra and comparing the  $x = 0.70$  glass spectrum to the spectra for both crystalline  $\text{Na}_2\text{CO}_3$  and  $x = 0.65$  glass, two distinct carbonate environments are clearly observed, see Figure 4. Pure  $\text{Na}_2\text{CO}_3$  presents one narrow peak, centered at 170.8 ppm, whereas the  $x = 0.65$  glass presents a broad peak, centered at 171.6 ppm. However, the  $x = 0.70$  glass presents both a narrow peak at 170.9 ppm and a broad peak at 171.5 ppm, see Figures 4 and 5. These chemical shifts and linewidths are consistent with previously measured crystalline sodium carbonate<sup>11</sup> and free sodium carbonate species<sup>9</sup>. This result implies that the  $x = 0.70$  glass contains both locally-ordered and locally-disordered carbonate environments. The  $\text{Na}_2\text{O-SiO}_2$  glasses in the range  $x = 0.40$  to  $x = 0.65$  only present the broad, locally-disordered carbonate environment, as shown in Figure 5.

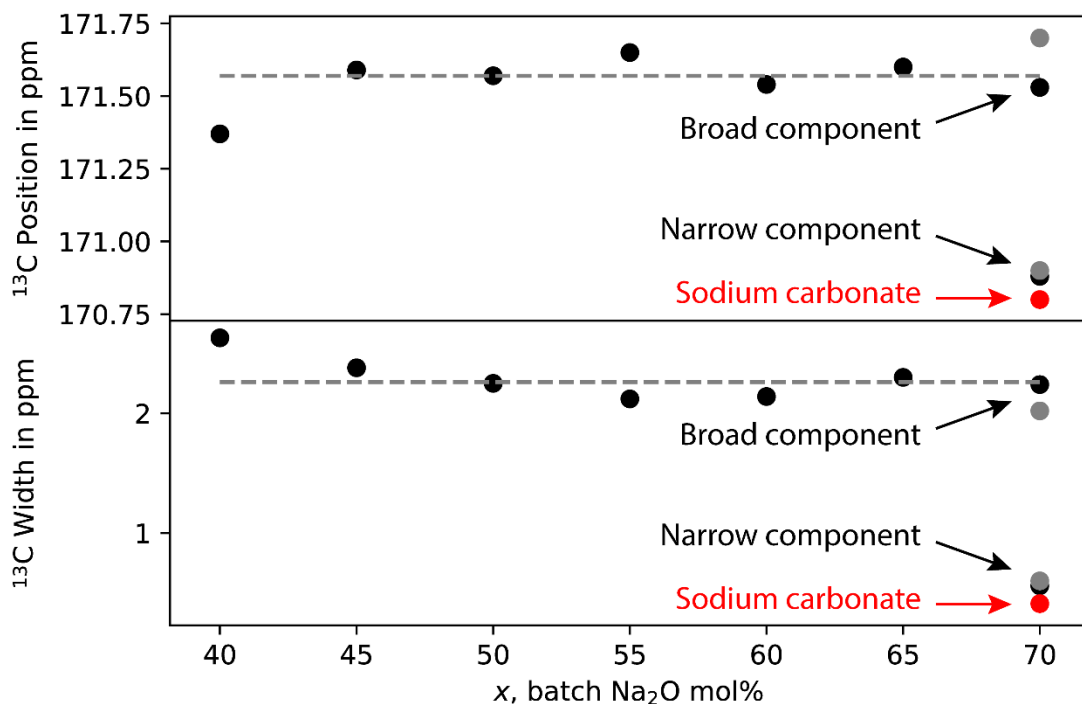


Figure 5. Fit parameters from  $^{13}\text{C}$  MAS-NMR for  $\text{Na}_2\text{O-SiO}_2$  glasses (black circles) and  $\text{Na}_2\text{CO}_3$  (red circles, arbitrarily placed at 70 mol%  $\text{Na}_2\text{O}$  for comparison). Two data points for each component at 70 mol%  $\text{Na}_2\text{O}$  show the variation in fitting results if different Gaussian:Lorentzian (G/L) ratios are used. The black dots are the same as the other compositions where all peaks are fixed to be Gaussian. The grey dots present a best fit with G/L ratio of 0.74 (broad peak) and 0.48 (narrow peak). The dashed line is the mean of the broad fit parameters.

The normalized (by mass)  $^{23}\text{Na}$  MAS-NMR spectra from  $x = 20$  mol% to  $x = 70$  mol% soda are shown in Figure 6. As expected, the  $^{23}\text{Na}$  signal from the glasses intensifies with  $\text{Na}_2\text{O}$  content, simply because more sodium is present. The line shapes are broad, indicating all sodium is

present in a locally disordered form (note the fast relaxation time used). As the relatively high magnetic field of 14.1 T was used, the peak widths are predominately due to the distribution of chemical shifts, rather than second-order quadrupolar broadening<sup>11</sup>.

Also observed is a systematic change in chemical shift to higher ppm (leftwards in Figure 6) as Na<sub>2</sub>O content increases in the glasses. This is consistent with a shortening of the average Na—O bond length from approximately 2.80 Å to 2.56 Å<sup>12-14</sup>. For low-Na<sub>2</sub>O glasses, and considering a Na<sup>+</sup> ion, the probability is high that a neighboring O<sup>-</sup> will be bonded to one or two Si<sup>4+</sup>. This Si—O covalent bond is stronger than the Na—O ionic bond, thus the oxygen will be much closer to silicon, especially where the oxygen is bridging two silicon atoms. For high-Na<sub>2</sub>O glasses the probability is now much lower that neighboring O<sup>-</sup> will be bonded to a silicon atom, rather the probability much higher that the neighboring O<sup>-</sup> will be non-bridging and not-bonded to a silicon.

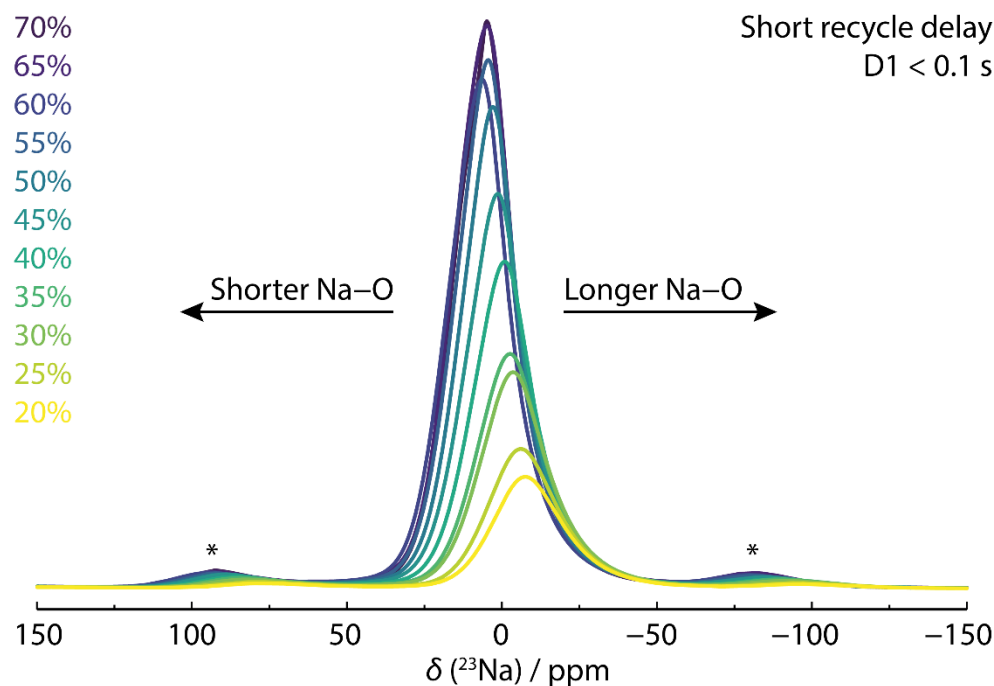


Figure 6. Normalized (by mass) <sup>23</sup>Na MAS NMR spectra at 14.1 T of sodium silicate glasses for 20 mol% to 70 mol% soda. Asterisks indicate spinning sidebands. Spectra acquired with a fast recycle delay.

Thus, as the coordination of sodium decreases a given Na<sup>+</sup> ion will have a slightly stronger, and therefore shorter, bond with the O<sup>-</sup>. In NMR, when there are less electrons near the nucleus (e.g., a nearby oxygen atom is withdrawing them), this manifests as a chemical shift to higher ppm. Interestingly, as is often the case for amorphous materials, this change proceeds smoothly, at least for compositions between  $x = 0.20$  to  $x = 0.60$ , see Figure 7. However, for compositions  $x = 0.65$  and  $x = 0.70$ , the shift reverses. These very high Na<sub>2</sub>O content glasses contain significant quantities of carbonate in their structure. As the carbon atom covalently bonds to its neighboring

oxygen atoms, they are pulled further away from the next-nearest neighboring Na<sup>+</sup> ions, hence the measured lengthening of the average Na—O bonds.

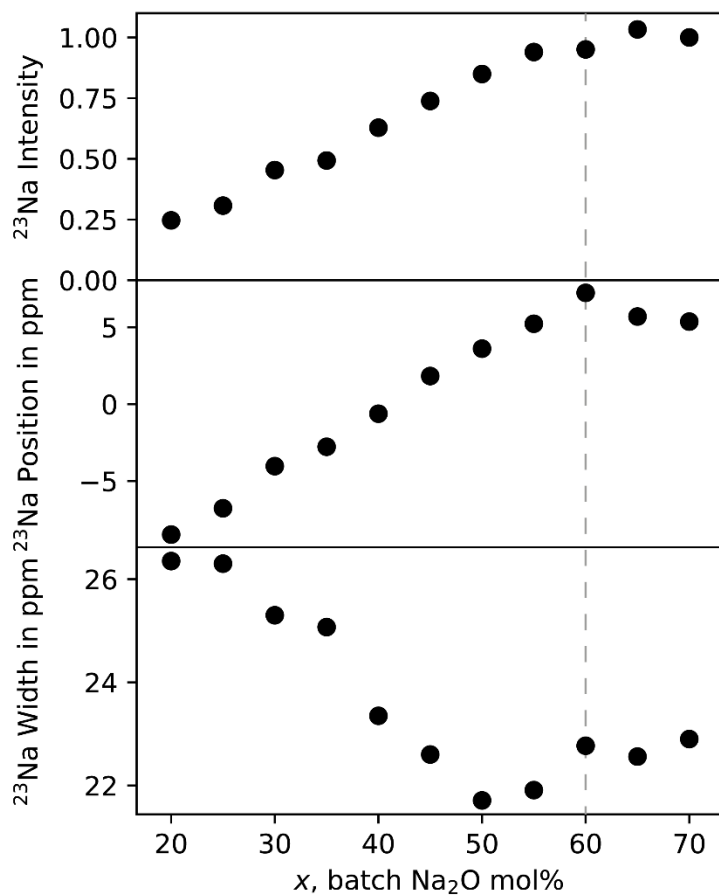


Figure 7. Selected fit parameters from <sup>23</sup>Na MAS-NMR for sodium silicate glasses obtained from DMFit<sup>15</sup>, with additional parameters given in Table 3. Pseudo-Voigt line shapes with chemical shift anisotropy were used as an approximate fit for each spectrum as a full fit would require modelling continuous distributions of both chemical shift and quadrupolar coupling. Intensity corresponds to normalized (by mass and number of scans) peak integral. Grey dashed line indicates x = 0.60, where the trend of peak position changes direction.

Batch xNa <sub>2</sub> O Composition (Mol. Fraction)	Amplitude	Position (ppm)	Width (ppm)	G/L ratio	CSA (ppm)	CSA eta	Integral [abs]
0.70	1.62E+09	5.37	22.90	0.64	-50.45	0.02	3.02E+14
0.65	1.57E+09	5.70	22.56	0.62	-45.67	0.89	3.12E+14

0.60	1.57E+09	7.24	22.77	0.57	-46.10	0.77	2.87E+14
0.55	1.5E+09	5.23	21.91	0.55	-44.33	0.66	2.84E+14
0.50	1.42E+09	3.61	21.71	0.55	-45.93	0.43	2.56E+14
0.45	1.12E+09	1.83	22.60	0.54	-51.40	0.55	2.23E+14
0.40	1.01E+09	-0.62	23.35	0.56	-51.61	0.38	1.9E+14
0.35	7.53E+08	-2.77	25.07	0.60	-56.46	0.84	1.49E+14
0.30	6.43E+08	-4.03	25.30	0.60	-53.41	0.84	1.37E+14
0.25	4.28E+08	-6.77	26.30	0.63	-59.64	0.74	9.27E+13
0.20	3.12E+08	-8.48	26.35	0.61	-56.28	0.88	7.44E+13

Table 3.  $^{23}\text{Na}$  MAS-NMR fit parameters. G/L is the ratio of the Gaussian intensity to Lorentzian. CSA is chemical shift anisotropy

The spectra shown in Figure 6 were deliberately measured using a fast relaxation time (0.01 s) to view the locally disordered component of the glasses only. When a longer relaxation time is used (10 s), the spectra appear as shown in Figure 8. For compositions  $x = 0.60$  and  $0.65$  the spectra are similar to the fast relaxation spectra, confirming that all of the sodium is present in the locally disordered phase. However, the spectrum for  $x = 0.70$  shows two additional sharp peaks superimposed over the locally disordered peak, consistent with the presence of two different sodium-containing phases. These additional peaks can be assigned to  $\text{Na}_2\text{CO}_3$  by comparison with the  $\text{Na}_2\text{CO}_3$  reference spectrum also shown in Figure 8.

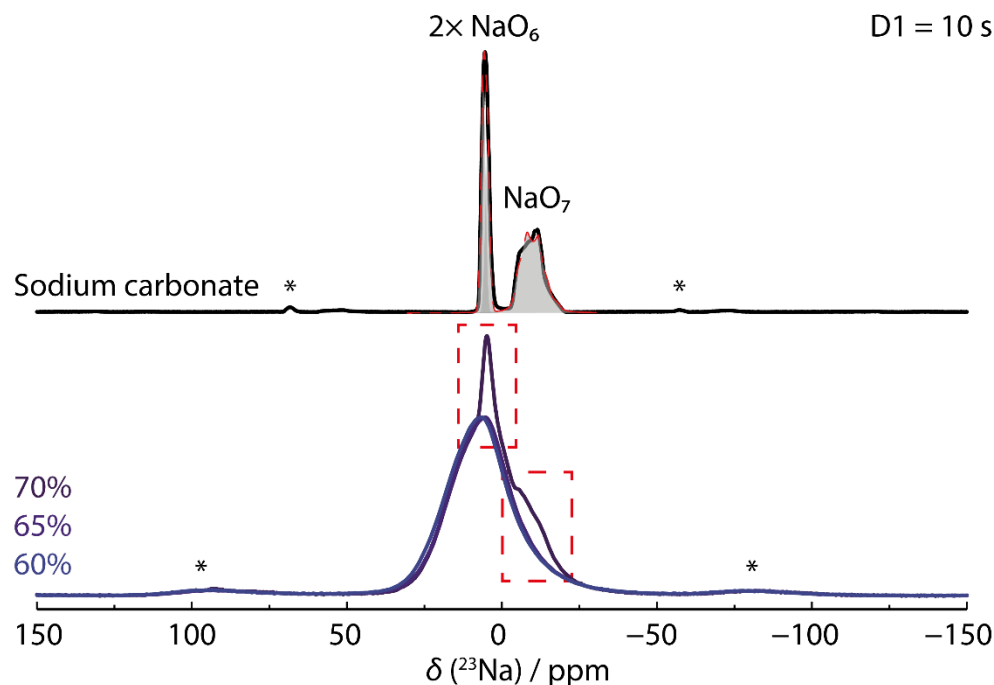


Figure 8.  $^{23}\text{Na}$  MAS-NMR spectra of crystalline  $\text{Na}_2\text{CO}_3$  and three high  $\text{Na}_2\text{O}$  content glasses. Asterisks indicate spinning sidebands. Spectra acquired with a slow recycle delay. Red dashed boxes indicate locally ordered sodium carbonate presence in the  $x = 0.70$  glass. Deconvolutions of  $^{23}\text{Na}$  Na signal from the sodium carbonate crystal are shown in grey. Spectra are not normalized, but scaled to the same height.

From the literature, we can assign the  $^{23}\text{Na}$  peaks of sodium carbonate<sup>16-17</sup>. Two spherically symmetric octahedral sites share the leftmost peak ( $\delta_{\text{iso}}$  between 5 ppm and 6.5 ppm), whereas the rightmost line shape ( $\delta_{\text{iso}} = 3.4$  ppm) is from a third sodium ion neighboring to seven oxygen ions. This lack of spherical symmetry causes its peak shape to become broadened by the quadrupolar interaction ( $C_Q = 2.4$  MHz,  $\eta_Q = 0.5$ ). A deconvolved spectrum showing these three sites is given in Figure 8.

#### IV. Discussion

The results presented here greatly add to our knowledge of sodium silicate glasses. We have been able to detect carbonate retention, a ubiquitous effect in modified oxide glasses prepared using conventional raw materials, in the form of a useable  $^{13}\text{C}$  symmetric MAS-NMR line shape, which indicates that the carbonate is locally disordered. We detected this signal even at  $J = 0.67$  (40 molar percent  $\text{Na}_2\text{O}$ ). According to the carbon assay results shown in Figure 1, the weight fraction of carbonate in this glass was just 0.001, i.e. 0.1 wt. %.

Understanding the factors and relationships governing the solubility of  $\text{CO}_2$  in silicate melts, and the behavior of carbonate melts (some of which are also glass-forming) holds great interest across a wide range of fields<sup>18-26</sup>. Geologists<sup>20-23,25,26</sup> have carried out many studies of  $\text{CO}_2$  in silicate glasses and melts, usually under high (GPa) applied pressures, and often in the presence of  $\text{H}_2\text{O}$ , in order to simulate deep geological conditions. Whilst our study here was not

specifically designed, or experimental conditions constrained, to provide CO<sub>2</sub> saturation of the melts, our results are nevertheless relevant. In particular, it has been shown that in some cases, carbon retention (as CO<sub>2</sub> or CO<sub>3</sub><sup>2-</sup>) in silicate melts yields linear relationships when plotted against the non-bridging oxygen per tetrahedron (NBO/T) ratio of the glass or melt<sup>25</sup>. Plotting NBO/T (calculated as 2[Na<sub>2</sub>O]/[SiO<sub>2</sub>], neglecting the repolymerising effect of the CO<sub>3</sub> groups) vs. carbon content of our glasses, shows a very similar relationship to that shown in Figure 1 see Figure 9. This non-linear relationship is markedly different from those obtained, for example, by Brooker *et al.*<sup>25</sup> for multicomponent melts under high (GPa) applied pressures where a number of linear relationships were obtained. A linear approximation can, however, be obtained by plotting the logarithm of carbon content against NBO/T, this is shown in Figure 9.

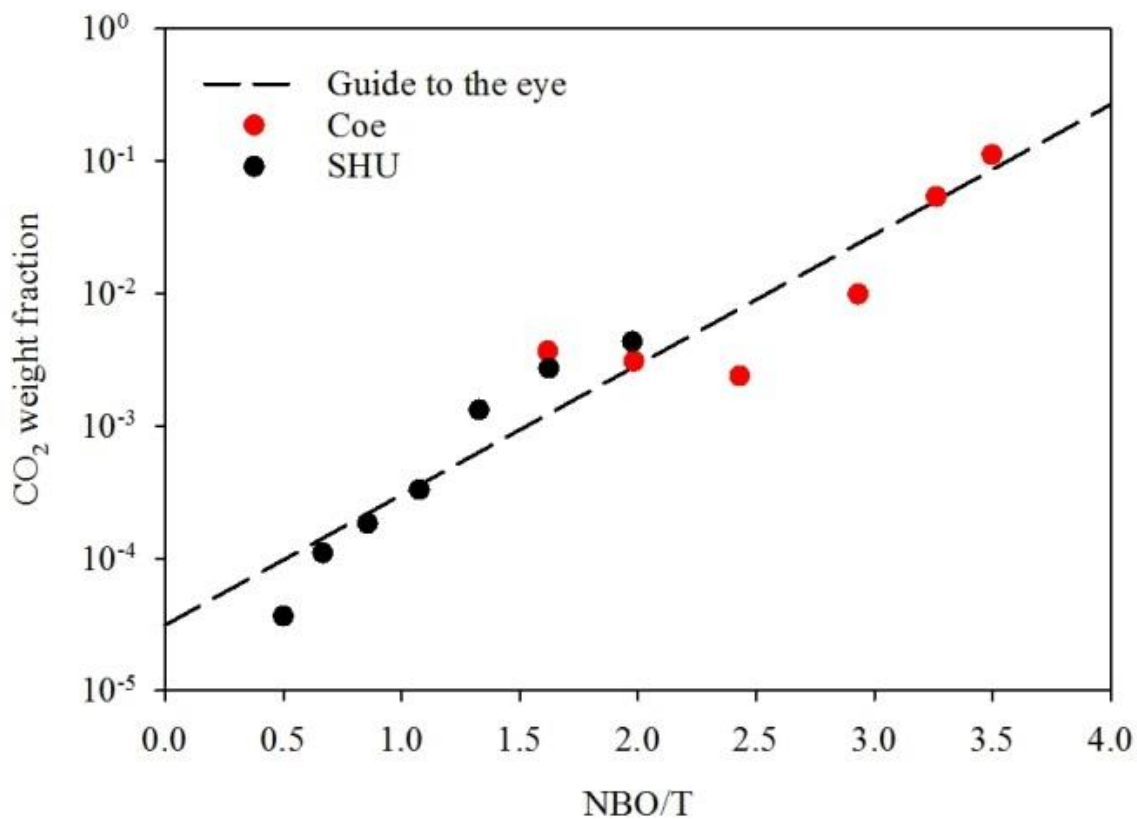


Figure 9: Carbon dioxide weight fraction as a function of fraction of non-bridging oxygen to tetrahedron ratio. The dashed line is a guide to the eye.

This behavior and its structural origins / relationships will be considered in detail in a forthcoming publication, however, it is worthwhile also briefly considering it here. The glasses studied here were prepared at atmospheric pressure, ~0.1 MPa or ~0.0001 GPa. Comparisons against data obtained for glasses prepared under pressure must be made carefully. Brooker *et al.*<sup>25</sup> showed an interesting relationship between CO<sub>2</sub> solubility and a very wide range of NBO/T (0 to 4), whereby at 2.0 GPa pressure an approximately linear relationship existed between CO<sub>2</sub> solubility and NBO/T, but at 0.2 GPa pressure this relationship has a sigmoid shape, whereby at lower NBO/T there is a lag in the increase of CO<sub>2</sub> solubility with NBO/T, and it does not begin



to increase significantly (when plotted on a linear scale) until  $\text{NBO}/\text{T} \sim 1$ . It is conceivable that such pressure-related behavior as highlighted by Brooker *et al.*<sup>25</sup> led to a similar but stronger sigmoid behavior for our samples (melted at 0.0001 GPa), whereby the  $\text{CO}_2$  solubility does not begin to increase strongly until  $\text{NBO}/\text{T} = 2$  to 3 (see Figure 1). This will be discussed further, in a structural context, in a forthcoming publication.

The  $^{13}\text{C}$  and  $^{23}\text{Na}$  MAS-NMR results for glasses with nominal compositions between 20 and 65 mol%  $\text{Na}_2\text{O}$  show broad, featureless, mostly Gaussian peaks. This indicates that both carbon (in the form of free sodium carbonate species) and  $\text{Na}^+$  ions are present in locally disordered environments. This implies that the  $\text{CO}_3^{2-}$  ions are necessarily surrounded by  $\text{Na}^+$  ions, forming nanoscale domains within the sodium silicate glass network. These nanoscale domains are small enough (perhaps only a single carbonate unit) to have a range of bond lengths and angles, appearing amorphous in form. However, for the 70 mol%  $\text{Na}_2\text{O}$  sample, both  $^{13}\text{C}$  and  $^{23}\text{Na}$  MAS-NMR reveal that some ( $< 30\%$ ) of the sodium is present in well-ordered  $\text{Na}_2\text{CO}_3$  units. This abundance indicates that a larger domain size of  $\text{Na}_2\text{CO}_3$  is present, distinct from the locally disordered sodium carbonate nanoscale domains. Supporting evidence comes from neutron scattering, the full details of which will be published in an associated paper. The neutron diffraction pattern of the sample with 70 mol%  $\text{Na}_2\text{O}$  shows some small Bragg peaks, arising from particles of crystalline  $\gamma\text{-Na}_2\text{CO}_3$  of diameter  $\sim 100$  Å, forming  $\sim 2\%$  of the sample, see Figure 10.

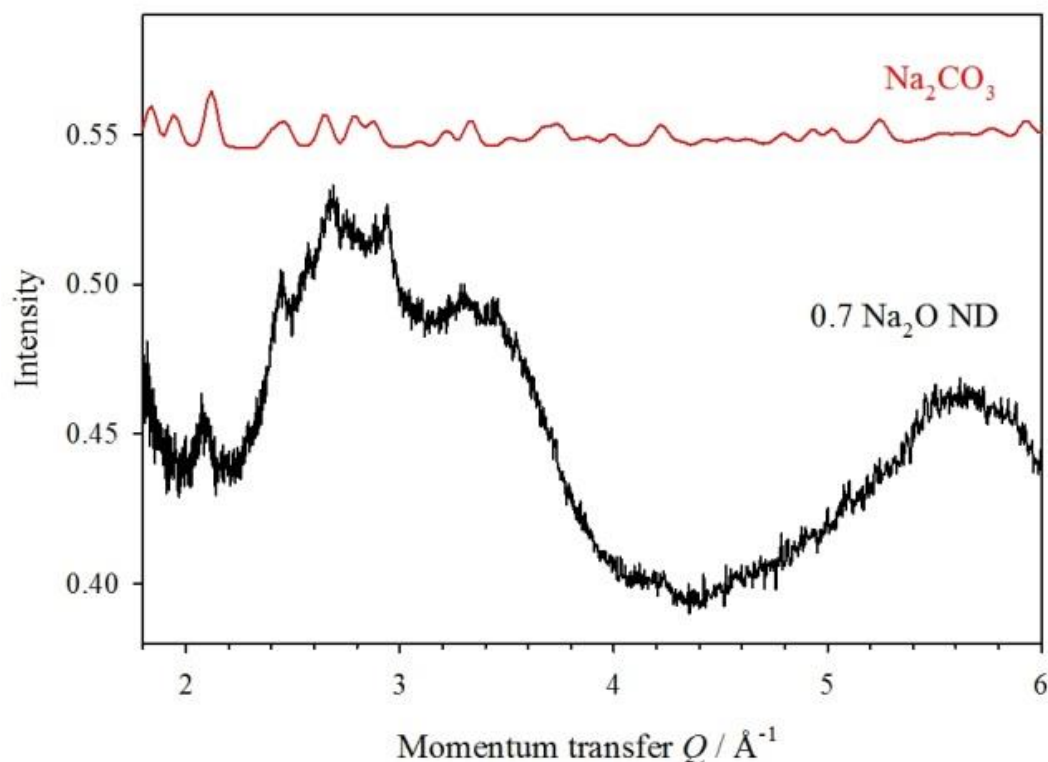


Figure 10. Neutron diffraction pattern for the 70 mol%  $\text{Na}_2\text{O}$  sample (black), together with a simulation for 100 Å crystallites of  $\gamma\text{-Na}_2\text{CO}_3$ , forming 2% of the sample.

Therefore, we propose that for smaller Na<sub>2</sub>O contents the CO<sub>3</sub> groups occur as individual structural entities that are isolated from each other, but for 70 mol% Na<sub>2</sub>O there is a significant number of CO<sub>3</sub> groups that occur in a cluster within the glass network, separated from each other only by Na<sup>+</sup> ions, with a similar arrangement at the local scale to that in crystalline Na<sub>2</sub>CO<sub>3</sub>, but without the occurrence of long range order. Potentially, longer melting times may reduce or eliminate these inclusions<sup>27</sup>, or perhaps between 65 and 70 mol% Na<sub>2</sub>O represents the maximum solubility limit for CO<sub>3</sub><sup>2-</sup> ions under the preparation conditions used here.

Comparison of our <sup>13</sup>C MAS-NMR results with data for other sodium-bearing glasses yields further insight into the structure of our glasses and the local environments of carbon and sodium. Kohn *et al.*<sup>28</sup> and Brooker *et al.*<sup>29</sup> studied a series of sodium aluminosilicate and sodium-calcium aluminosilicate melts and glasses prepared under pressures of 1 to 2.5 GPa. Kohn *et al.*'s<sup>28</sup> NaAlSiO<sub>4</sub> glass gave an asymmetric peak centered at ~163 ppm with additional, weaker components towards lower chemical shifts, creating asymmetry in the overall band. Conversely, their soda-melilite (CaNaAlSi<sub>2</sub>O<sub>7</sub>) glass provided a single, symmetrical peak centered at ~168 ppm. For the sodium aluminosilicates, Brooker *et al.*<sup>29</sup> found similar asymmetric peaks to Kohn *et al.*<sup>28</sup>, again centered at ~163-165 ppm with a tail towards lower chemical shifts creating the asymmetry. They attributed these contributions to different species of “network carbonate” units, including Si-carbonate-Al and Al-carbonate-Al units. Brooker *et al.*<sup>29</sup> noted a weak peak at 171-175 ppm, suggesting that it may be related to a small amount of Na-carbonate ionic complexes present in their glasses. Recently Xue *et al.*<sup>30</sup> found results consistent with Brooker *et al.*<sup>29</sup> and expanded upon their findings.

Kim *et al.*<sup>31</sup> recently used <sup>13</sup>C MAS-NMR to study Na<sub>2</sub>O·3SiO<sub>2</sub> glasses prepared under a range of pressures from 4 to 8 GPa, and found that the CO<sub>3</sub><sup>2-</sup> free carbonate peak near 170 ppm shifted to lower frequency with increasing pressure, with the peak positions from 171.7 ppm at 4 GPa to 170.2 ppm at 8 GPa. Our corresponding Na<sub>2</sub>O·3SiO<sub>2</sub> glass ( $x = 0.25$ ) contained extremely low (0.003 wt%) carbon and consequently we were unable to obtain an NMR signal. However, due to being prepared under high pressure, Kim *et al.*'s<sup>31</sup> glass contained 0.09 – 0.27 wt % <sup>13</sup>CO<sub>2</sub> and thus they obtained a <sup>13</sup>C MAS-NMR signal, albeit with a modest signal-to-noise ratio. The absence of any peaks at ~160-165 ppm in the spectra for all glasses studied here (Figure 3) also confirms the absence of bridging carbonates such as <sup>141</sup>Si(CO<sub>3</sub>)<sup>141</sup>Si or the network carbonate units described by Brooker *et al.*<sup>29</sup> and Xue *et al.*<sup>30</sup>. Such units were also observed by Kim *et al.*<sup>31</sup> in their Na<sub>2</sub>O·3SiO<sub>2</sub> melts, but only at pressures of 6 GPa and above. Such network carbonate units are therefore not expected in sodium silicate glasses melted at ambient pressures, and the absence of peaks at ~160-165 in our <sup>13</sup>C MAS-NMR spectra (Figure 3) confirms this. It can therefore be confidently demonstrated that essentially all carbon in all samples studied here is present in the form of ionic CO<sub>3</sub><sup>2-</sup> units. As noted previously, we can conclude that these CO<sub>3</sub><sup>2-</sup> units are surrounded by Na<sup>+</sup> ions, forming nanoscale domains within the sodium silicate glass network.

For the first time, we have prepared and studied sodium silicate glasses across a very wide range of compositions, from (mol%, nominal) 20Na<sub>2</sub>O·80SiO<sub>2</sub> to 70Na<sub>2</sub>O·30SiO<sub>2</sub>, in incremental steps of 5 mol%. This, and our other work on these glasses, soon to be published, augments and expands upon previous work including the highly-cited 1991 paper by Maekawa *et al.*<sup>4</sup> The glass

formation region within the Na<sub>2</sub>O-SiO<sub>2</sub> system that is readily accessible to standard melt-pour glassmaking approaches ends at 50-55 mol% Na<sub>2</sub>O, as we have demonstrated here, and as also indicated by Maekawa *et al.*<sup>4</sup>, who quenched their melts in water or liquid N<sub>2</sub>. Only by extremely rapid quenching, accessed in this study by our novel roller-quench apparatus, has it been possible to access glasses with very high Na<sub>2</sub>O contents of up to 70 mol%. In so doing, we have established new information on this archetypal yet simple glass-forming system. Crucially, we have shown that this “traditional” glass-formation boundary of approximately 50-55 mol% Na<sub>2</sub>O also represents the point at which, from a structural and technological perspective, CO<sub>2</sub> retention as carbonate achieves significant levels (0.5 weight %) and then rapidly increases with further increases in nominal Na<sub>2</sub>O content of the glass. This is also the nominal Na<sub>2</sub>O content above which the carbonate anions are sufficiently abundant so as to have significant structural impacts on the glass, as evidenced by the changes we observe in the peak widths and positions in <sup>23</sup>Na MAS-NMR spectra (Figure 7).

Furthermore, neutron and X-ray diffraction experiments have been carried out, and will be reported in a future publication, which will describe the structural changes that take place over this wide range of compositions. It will also examine carbonate retention in terms of abundance, amorphous character, bond lengths, and bond angles. Further, the sodium-oxygen bond character will be presented. Also, a paper is in preparation detailing results from <sup>29</sup>Si MAS-NMR, Raman spectroscopy, thermal property analysis and density measurements. The three papers will present a thorough view of the various structural changes taking place in this most important glass system.

Our results therefore have implications for multiple fields of research. First, in carbonate glass-forming systems, geological melts, liquids and volatiles<sup>18-23,25,26</sup> as our results provide important information on structural changes upon incorporation and retention of large amounts of carbonate in silicate melts and glasses prepared under atmospheric pressures, unlike previous studies conducted under pressure. In particular, we see evidence from both carbon and sodium MAS-NMR for glassy carbonate in at least two structural roles in the highest Na<sub>2</sub>O-content glasses. Second, in glass science<sup>4,8-14</sup> as our results extend the established range of the Na<sub>2</sub>O-SiO<sub>2</sub> glass-forming system and show structural and compositional evolution as a result of carbonate incorporation. Third, in glass technology<sup>24</sup> as our results show that stable carbonate-rich glasses can be produced at the extreme ends of the simple glass-forming systems on which many technological glasses are based that retain only parts-per-million levels of CO<sub>2</sub> (e.g. commercial Na<sub>2</sub>O-CaO-SiO<sub>2</sub> glass systems), implying opportunities for enhanced carbonate incorporation in technological glass-forming systems and potentially providing new glass properties and functionalities, also with potential for future carbon capture opportunities.

## V. Conclusions

Sodium environments and carbonate retention in the widest-yet-studied compositional range of Na<sub>2</sub>O-SiO<sub>2</sub> glasses were investigated using a range of complementary quantitative means. These included multinuclear nuclear magnetic resonance and carbon elemental assay. The results show CO<sub>3</sub><sup>2-</sup> retention beginning with trace amounts at 40 mol% Na<sub>2</sub>O (elemental analysis) and <sup>13</sup>C NMR detection at 40 mol% Na<sub>2</sub>O. Based on our <sup>23</sup>Na MAS NMR results, Na-O bond lengths

decrease linearly with increasing Na<sub>2</sub>O content of the glasses, up to 60 mol% Na<sub>2</sub>O. Carbonate retention accelerates greatly with increasing Na<sub>2</sub>O contents above 60 mol%. The carbonate anions are necessarily surrounded by Na<sup>+</sup> ions, and are shown to be present in a form of dissolved, locally disordered, nanoscale domains. At 70 mol% Na<sub>2</sub>O the weight fraction of carbonate in the glass exceeds 15%. Results from both <sup>13</sup>C and <sup>23</sup>Na MAS-NMR are consistent with the 70 mol% Na<sub>2</sub>O glass containing both short-range ordered sodium carbonate and amorphous sodium carbonate environments.

## VI. Acknowledgements

M.P., M.A. and S.F. thank the US National Science Foundation for supporting this work under grant number NSF-DMR 1746230. M.C.W and P.A.B. acknowledge with thanks support from EPSRC under grant EP/R036225/1.

## VII. References

1. F. Baino, Bioactive glasses – When glass science and technology meet regenerative medicine, *Ceramics International*, 2018, **44**, 14953-14966. <https://doi.org/10.1016/j.ceramint.2018.05.180>
2. E. Axinte, Glasses as engineering materials: A review, *Materials & Design*, 2011, **32**, 1717-1732. <https://doi.org/10.1016/j.matdes.2010.11.057>
3. S. Prasad, T. M. Clark, T. H. Sefzik, H.-T. Kwak, Z. Gan and P. J. Grandinetti, Solid-state multinuclear magnetic resonance investigation of Pyrex(R), *Journal of Non-Crystalline Solids*, 2006, **352**, 2834-2840. <https://doi.org/10.1016/j.jnoncrysol.2006.02.085> Doi:
4. H. Maekawa, T. Maekawa, K. Kawamura and T. Yokokawa, The structural groups of alkali silicate glasses determined from <sup>29</sup>Si MAS-NMR, *Journal of Non-Crystalline Solids*, 1991, **127**, 53-64. [https://doi.org/10.1016/0022-3093\(91\)90400-Z](https://doi.org/10.1016/0022-3093(91)90400-Z)
5. H. Zhang, S. Koritala, K. Farooqui, R. Boekenhauer, D. Bain, S. Kambeyanda, and S. Feller, A Model for Carbon Retention Dioxide Retention in Alkali Borate and Borosilicate Systems, *Physics and Chemistry of Glasses*, 1991, **32**(5), 185-187
6. J.Kasper, S. Feller, and G.Sumcad, New Sodium-Borate Glasses, *Journal of American Ceramic Society*, 1984, **67** No. 4 C-71
7. S.W. Martin and C.A. Angell, Glass formation and transition temperatures in sodium and lithium borate and aluminoborate melts up to 72 mol.% alkali, *Journal of Non-Crystalline Solids*, 1984, **66**, 429-442. [https://doi.org/10.1016/0022-3093\(84\)90368-5](https://doi.org/10.1016/0022-3093(84)90368-5)
8. M. G. Mortuza, R. Dupree and D. Holland, Studies of the effect of paramagnetic impurity in the structure of sodium disilicate glass, *Journal of Materials Science*, 2000, **35**, 2829-2832. <https://doi.org/10.1023/a:1004751303503>
9. X. Xue, M. Kanzaki, P. Flourey, T. Tobase and J. Eguchi, Carbonate speciation in depolymerized and polymerized (alumino)silicate glasses: Constraints from <sup>13</sup>C MAS and static NMR measurements and ab initio calculations, *Chemical Geology*, 2018, **479**, 151-165. <https://doi.org/10.1016/j.chemgeo.2018.01.005>
10. C. Dybowski, E. J. Gaffney, A. Sayir and M. J. Rabinowitz, Solid-state <sup>13</sup>C and <sup>29</sup>Si MAS NMR spectroscopy of silicon carbide, *Colloids and Surfaces A: Physicochemical and Engineering Aspects*, 1996, **118**, 171-181. [https://doi.org/10.1016/0927-7757\(96\)03735-1](https://doi.org/10.1016/0927-7757(96)03735-1)

11. A. R. Jones, R. Winter, G. N. Greaves and I. H. Smith,  $^{23}\text{Na}$ ,  $^{29}\text{Si}$ , and  $^{13}\text{C}$  MAS NMR Investigation of Glass-Forming Reactions between  $\text{Na}_2\text{CO}_3$  and  $\text{SiO}_2$ , *The Journal of Physical Chemistry B*, 2005, **109**, 23154-23161. <https://doi.org/10.1021/jp053953y>
12. S. K. Lee and J. F. Stebbins, The distribution of sodium ions in aluminosilicate glasses: a high-field Na-23 MAS and 3Q MAS NMR study, *Geochimica Et Cosmochimica Acta*, 2003, **67**, 1699-1709. [https://doi.org/10.1016/s0016-7037\(03\)00026-7](https://doi.org/10.1016/s0016-7037(03)00026-7)
13. X. Xue and J. F. Stebbins,  $^{23}\text{Na}$  NMR chemical shifts and local Na coordination environments in silicate crystals, melts and glasses, *Physics and Chemistry of Minerals*, 1993, **20**, 297-307. <https://doi.org/10.1007/bf00215100>
14. J. F. Stebbins, Cation sites in mixed-alkali oxide glasses: correlations of NMR chemical shift data with site size and bond distance, *Solid State Ionics*, 1998, **112**, 137-141. [https://doi.org/10.1016/s0167-2738\(98\)00224-0](https://doi.org/10.1016/s0167-2738(98)00224-0)
15. D. Massiot, F. Fayon, M. Capron, I. King, S. Le Calvé, B. Alonso, J. O. Durand, B. Bujoli, Z. Gan, G. Hoatson, 'Modelling one and two-dimensional solid-state NMR spectra.', *Magn. Reson. Chem.* 40 70-76 (2002) doi:10.1002/mrc.984
16. Z. E. M. Reeve, C. J. Franko, K. J. Harris, H. Yadegari, X. Sun and G. R. Goward, Detection of Electrochemical Reaction Products from the Sodium–Oxygen Cell with Solid-State  $^{23}\text{Na}$  NMR Spectroscopy, *Journal of the American Chemical Society*, 2017, **139**, 595-598. <https://doi.org/10.1021/jacs.6b11333>
17. G. Chapuis, M. Dusek, M. Meyer and V. Petricek, Sodium carbonate revisited, *Acta Crystallographica Section B*, 2003, **59**, 337-352. <https://doi.org/10.1107/s0108768103009017>
18. M. Wilding, P. A. Bingham, M. Wilson, Y. Kono, J. W. E. Drewitt, R. A. Brooker and J. B. Parise,  $\text{CO}_{3+1}$  network formation in ultra-high pressure carbonate liquids, *Scientific Reports*, 2019, **9**, 15416.
19. M. Wilding, B. L. Phillips, M. Wilson, G. Sharma, A. Navrotsky, P. A. Bingham, R. Brooker and J. B. Parise, The structure and thermochemistry of  $\text{K}_2\text{CO}_3 - \text{MgCO}_3$  glass, *Journal of Materials Research*, 2019, **34**, 3377-3388.
20. A. P. Jones, M. Genge and L. Carmody, Carbonate melts and carbonatites. In Carbon in Earth, R. M. Hazen, A. P. Jones, and J. A. Baross, eds., The Mineralogical Society of America, Chantilly, Virginia, 2013, pp. 289–322.
21. J. G. Blank and R. A. Brooker, Experimental studies of carbon dioxide in silicate melts: solubility, speciation and stable carbon isotope behaviour, in Reviews in Mineralogy, Volatiles in Magmas, M. R. Carroll and J. R. Holloway, eds., The Mineralogical Society of America, Washington D. C., 1994, 30, pp. 157-186.
22. J. R. Holloway and J. G. Blank, Application of experimental results to C-O-H species in natural melts, in Reviews in Mineralogy, Volatiles in Magmas, M. R. Carroll and J. R. Holloway, eds., The Mineralogical Society of America, Washington D. C., 1994, 30, pp. 187-230.
23. R. A. Lange, The effect of  $\text{H}_2\text{O}$ ,  $\text{CO}_2$  and F on the density and viscosity of silicate melts, in Reviews in Mineralogy, Volatiles in Magmas, M. R. Carroll and J. R. Holloway, eds., The Mineralogical Society of America, Washington D. C., 1994, 30, pp. 331-370.
24. F. T. Wallenberger and P. A. Bingham, Eds, Fiberglass and glass technology: energy-friendly compositions and applications, Springer, New York, 2010, 451 pages.

25. R. A. Brooker, S. C. Kohn, J. R. Holloway and P. F. McMillan, Structural controls on the solubility of CO<sub>2</sub> in silicate melts Part I: bulk solubility data, *Chemical Geology*, 2001, **174**, 225-239.
26. H. Ni and H. Keppler, Carbon in silicate melts, in Reviews in Mineralogy and Geochemistry, R. M. Hazen, A. P. Jones and J. A. Baross, eds., The Mineralogical Society of America, Washington D. C., 2013, 75, pp. 251-287.
27. A. R. Jones, R. Winter, P. Florian and D. Massiot, Tracing the Reactive Melting of Glass-Forming Silicate Batches by In Situ <sup>23</sup>Na NMR, *The Journal of Physical Chemistry B*, 2005, **109**, 4324-4332. <https://doi.org/10.1021/jp045705s>
28. S. C. Kohn, R. A. Brooker and R. Dupree, <sup>13</sup>C MAS NMR: A method for studying CO<sub>2</sub> speciation in glasses, *Geochimica et Cosmochimica Acta*, 1991, **55**, 3879-3884.
29. R. A. Brooker, S. C. Kohn, J. R. Holloway, P. F. McMillan and M. R. Carroll, Solubility, speciation and dissolution mechanisms for CO<sub>2</sub> in melts on the NaAlO<sub>2</sub>-SiO<sub>2</sub> join, *Geochimica et Cosmochimica Acta*, 1999, **63**, 3549-3565.
30. X. Xue, M. Kanzaki, P. Floury, T. Tobase and J. Eguchi, Carbonate speciation in depolymerized and polymerized (alumino)silicate glasses: Constraints from <sup>13</sup>C MAS and static NMR measurements and ab initio calculations, *Chemical Geology*, 2018, **479**, 151-165.
31. E. J. Kim, Y. Fei and S. K. Lee, Effect of pressure on the short-range structure and speciation of carbon in alkali silicate and aluminosilicate glasses and melts at high pressure up to 8 GPa: <sup>13</sup>C, <sup>27</sup>Al, <sup>17</sup>O and <sup>29</sup>Si solid-state NMR study, *Geochimica et Cosmochimica Acta*, 2018, **224**, 327-343.